Fermilab FERMILAB-Pub-02/097-E June 2002

Branching Ratio Measurements of Exclusive B^+ Decays to Charmonium with the Collider Detector at Fermilab

D. Acosta,[13] T. Affolder,[24] H. Akimoto,[47] M. G. Albrow,[12] D. Ambrose,[34] D. Amidei,[26] K. Anikeev,[25] J. Antos,[1] G. Apollinari,[12] T. Arisawa,[47] A. Artikov,[10] T. Asakawa,[45] W. Ashmanskas,[9] F. Azfar,[32] P. Azzi-Bacchetta,[33] N. Bacchetta,[33] H. Bachacou,[24] W. Badgett,[12] S. Bailey,[17] P. de Barbaro,[38] A. Barbaro-Galtieri,[24] V. E. Barnes,[37] B. A. Barnett,[20] S. Baroiant,[5] M. Barone,[14] G. Bauer,[25] F. Bedeschi,[35] S. Behari,[20] S. Belforte,[44] W. H. Bell,[16] G. Bellettini,[35] J. Bellinger,[48] D. Benjamin,[11] J. Bensinger,[4] A. Beretvas,[12] J. Berryhill,[9] A. Bhatti,[39] M. Binkley,[12] D. Bisello,[33] M. Bishai,[12] R. E. Blair,[2] C. Blocker,[4] K. Bloom,[26] B. Blumenfeld,[20] S. R. Blusk,[38] A. Bocci,[39] A. Bodek,[38] G. Bolla,[37] Y. Bonushkin,[6] D. Bortoletto,[37] J. Boudreau,[36] A. Brandl,[28] C. Bromberg,[27] M. Brozovic,[11] E. Brubaker,[24] N. Bruner,[28] J. Budagov,[10] H. S. Budd,[38] K. Burkett,[17] G. Busetto,[33] K. L. Byrum,[2] S. Cabrera,[11] P. Calafiura,[24] M. Campbell,[26] W. Carithers,[24] J. Carlson,[26] D. Carlsmith,[48] W. Caskey,[5] A. Castro,[3] D. Cauz,[44] A. Cerri,[35] A. W. Chan,[1] P. S. Chang,[1] P. T. Chang,[1] J. Chapman,[26] C. Chen,[34] Y. C. Chen,[1] M. -T. Cheng,[1] M. Chertok,[5] G. Chiarelli,[35] I. Chirikov-Zorin,[10] G. Chlachidze,[10] F. Chlebana,[12] L. Christofek,[19] M. L. Chu,[1] J. Y. Chung,[30] W. -H. Chung,[48] Y. S. Chung,[38] C. I. Ciobanu,[30] A. G. Clark,[15] M. Coca,[38] A. P. Colijn,[12] A. Connolly,[24] M. Convery,[39] J. Conway,[40] M. Cordelli,[14] J. Cranshaw,[42] R. Culbertson,[12] D. Dagenhart,[46] S. D'Auria,[16] F. DeJongh,[12] S. Dell'Agnello,[14] M. Dell'Orso,[35] S. Demers,[38] L. Demortier,[39] M. Deninno,[3] P. F. Derwent,[12] T. Devlin,[40] J. R. Dittmann,[12] A. Dominguez,[24] S. Donati,[35] M. D'Onofrio,[35] T. Dorigo,[17] I. Dunietz,[12] N. Eddy,[19] K. Einsweiler,[24] E. Engels, Jr.,[36] R. Erbacher,[12] D. Errede,[19] S. Errede,[19] Q. Fan,[38] H.-C. Fang,[24] R. G. Feild,[49] J. P. Fernandez,[37] C. Ferretti,[35] R. D. Field,[13] I. Fiori,[3] B. Flaugher,[12] L. R. Flores-Castillo,[36] G. W. Foster,[12] M. Franklin,[17] J. Freeman,[12] J. Friedman,[25] Y. Fukui,[23] I. Furic,[25] S. Galeotti,[35] A. Gallas,[29] M. Gallinaro,[39] T. Gao,[34] M. Garcia-Sciveres,[24] A. F. Garfinkel,[37] P. Gatti,[33] C. Gay,[49] D. W. Gerdes,[26] E. Gerstein,[8] P. Giannetti,[35] K. Giolo,[37] M. Giordani,[5] P. Giromini,[14] V. Glagolev,[10] D. Glenzinski,[12] M. Gold,[28] J. Goldstein,[12] G. Gomez,[7] I. Gorelov,[28] A. T. Goshaw,[11] Y. Gotra,[36] K. Goulianos,[39] C. Green,[37] G. Grim,[5] C. Grosso-Pilcher,[9] M. Guenther,[37] G. Guillian,[26] J. Guimaraes da Costa,[17] R. M. Haas,[13] C. Haber,[24] S. R. Hahn,[12] C. Hall,[17] T. Handa,[18] R. Handler,[48] F. Happacher,[14] K. Hara,[45] A. D. Hardman,[37] R. M. Harris,[12] F. Hartmann,[21] K. Hatakeyama,[39] J. Hauser,[6] J. Heinrich,[34] A. Heiss,[21] M. Herndon,[20] C. Hill,[5] A. Hocker,[38] K. D. Hoffman,[9] R. Hollebeek,[34] L. Holloway,[19] B. T. Huffman,[32] R. Hughes,[30] J. Huston,[27] J. Huth,[17] H. Ikeda,[45] J. Incandela,[(*) 12] G. Introzzi,[35] A. Ivanov,[38] J. Iwai,[47] Y. Iwata,[18] E. James,[26] M. Jones,[34] U. Joshi,[12] H. Kambara,[15] T. Kamon,[41] T. Kaneko,[45] M. Karagoz Unel,[29] K. Karr,[46] S. Kartal,[12] H. Kasha,[49] Y. Kato,[31] T. A. Keaffaber,[37] K. Kelley,[25] M. Kelly,[26] R. D. Kennedy,[12] R. Kephart,[12] D. Khazins,[11] T. Kikuchi,[45] B. Kilminster,[38] B. J. Kim,[22] D. H. Kim,[22] H. S. Kim,[19] M. J. Kim,[8] S. B. Kim,[22] S. H. Kim,[45] Y. K. Kim,[24] M. Kirby,[11] M. Kirk,[4] L. Kirsch,[4] S. Klimenko,[13] P. Koehn,[30] K. Kondo,[47] J. Konigsberg,[13] A. Korn,[25] A. Korytov,[13] E. Kovacs,[2] J. Kroll,[34] M. Kruse,[11] V. Krutelyov,[41] S. E. Kuhlmann,[2] K. Kurino,[18] T. Kuwabara,[45] A. T. Laasanen,[37] N. Lai,[9] S. Lami,[39] S. Lammel,[12] J. Lancaster,[11] M. Lancaster,[24] R. Lander,[5] A. Lath,[40] G. Latino,[28] T. LeCompte,[2] Y. Le,[20] K. Lee,[42] S. W. Lee,[41] S. Leone,[35] J. D. Lewis,[12] M. Lindgren,[6] T. M. Liss,[19] J. B. Liu,[38] T. Liu,[12] Y. C. Liu,[1] D. O. Litvintsev,[12] O. Lobban,[42] N. S. Lockyer,[34] J. Loken,[32] M. Loreti,[33] D. Lucchesi,[33] P. Lukens,[12] S. Lusin,[48] L. Lyons,[32] J. Lys,[24] R. Madrak,[17] K. Maeshima,[12] P. Maksimovic,[20] L. Malferrari,[3] M. Mangano,[35] G. Manca,[32] M. Mariotti,[33] G. Martignon,[33] M. Martin,[20] A. Martin,[49] V. Martin,[29] J. A. J. Matthews,[28] P. Mazzanti,[3] K. S. McFarland,[38] P. McIntyre,[41] M. Menguzzato,[33] A. Menzione,[35] P. Merkel,[12] C. Mesropian,[39] A. Meyer,[12] T. Miao,[12] R. Miller,[27] J. S. Miller,[26] H. Minato,[45] S. Miscetti,[14] M. Mishina,[23] G. Mitselmakher,[13] Y. Miyazaki,[31] N. Moggi,[3] E. Moore,[28] R. Moore,[26] Y. Morita,[23] T. Moulik,[37] M. Mulhearn,[25] A. Mukherjee,[12] T. Muller,[21] A. Munar,[35] P. Murat,[12] S. Murgia,[27] J. Nachtman,[6] V. Nagaslaev,[42] S. Nahn,[49] H. Nakada,[45] I. Nakano,[18] R. Napora,[20] C. Nelson,[12] T. Nelson,[12] C. Neu,[30] D. Neuberger,[21] C. Newman-Holmes,[12] C.-Y. P. Ngan,[25] T. Nigmanov,[36] H. Niu,[4] L. Nodulman,[2] A. Nomerotski,[13] S. H. Oh,[11] Y. D. Oh,[22] T. Ohmoto,[18] T. Ohsugi,[18] R. Oishi,[45] T. Okusawa,[31] J. Olsen,[48] W. Orejudos,[24] C. Pagliarone,[35] F. Palmonari,[35] R. Paoletti,[35]

V. Papadimitriou,[42] D. Partos,[4] J. Patrick,[12] G. Pauletta,[44] M. Paulini,[8] T. Pauly,[32] C. Paus,[25] D. Pellett,[5] L. Pescara,[33] T. J. Phillips,[11] G. Piacentino,[35] J. Piedra,[7] K. T. Pitts,[19] A. Pompos,[37] L. Pondrom,[48] G. Pope,[36] T. Pratt,[32] F. Prokoshin,[10] J. Proudfoot,[2] F. Ptohos,[14] O. Pukhov,[10] G. Punzi,[35] J. Rademacker,[32] A. Rakitine,[25] F. Ratnikov,[40] D. Reher,[24] A. Reichold,[32] P. Renton,[32] A. Ribon,[33] W. Riegler,[17] F. Rimondi,[3] L. Ristori,[35] M. Riveline,[43] W. J. Robertson,[11] T. Rodrigo,[7] S. Rolli,[46] L. Rosenson,[25] R. Roser,[12] R. Rossin,[33] C. Rott,[37] A. Roy,[37] A. Ruiz,[7] A. Safonov,[5] R. St. Denis,[16] W. K. Sakumoto,[38] D. Saltzberg,[6] C. Sanchez,[30] A. Sansoni,[14] L. Santi,[44] H. Sato,[45] P. Savard,[43] A. Savoy-Navarro,[12] P. Schlabach,[12] E. E. Schmidt,[12] M. P. Schmidt,[49] M. Schmitt,[29] L. Scodellaro,[33] A. Scott,[6] A. Scribano,[35] A. Sedov,[37] S. Seidel,[28] Y. Seiya,[45] A. Semenov,[10] F. Semeria,[3] T. Shah,[25] M. D. Shapiro,[24] P. F. Shepard,[36] T. Shibayama,[45] M. Shimojima,[45] M. Shochet,[9] A. Sidoti,[33] J. Siegrist,[24] A. Sill,[42] P. Sinervo,[43] P. Singh,[19] A. J. Slaughter,[49] K. Sliwa,[46] F. D. Snider,[12] A. Solodsky,[39] J. Spalding,[12] T. Speer,[15] M. Spezziga,[42] P. Sphicas,[25] F. Spinella,[35] M. Spiropulu,[9] L. Spiegel,[12] J. Steele,[48] A. Stefanini,[35] J. Strologas,[19] F. Strumia, [15] D. Stuart,[(*) 12] K. Sumorok,[25] T. Suzuki,[45] T. Takano,[31] R. Takashima,[18] K. Takikawa,[45] P. Tamburello,[11] M. Tanaka,[45] B. Tannenbaum,[6] M. Tecchio,[26] R. J. Tesarek,[12] P. K. Teng,[1] K. Terashi,[39] S. Tether,[25] A. S. Thompson,[16] E. Thomson,[30] R. Thurman-Keup,[2] P. Tipton,[38] S. Tkaczyk,[12] D. Toback,[41] K. Tollefson,[27] A. Tollestrup,[12] D. Tonelli,[35] M. Tonnesmann,[27] H. Toyoda,[31] W. Trischuk,[43] J. F. de Troconiz,[17] J. Tseng,[25] D. Tsybychev,[13] N. Turini,[35] F. Ukegawa,[45] T. Vaiciulis,[38] J. Valls,[40] E. Vataga,[35] S. Vejcik III,[12] G. Velev,[12] G. Veramendi,[24] R. Vidal,[12] I. Vila,[7] R. Vilar,[7] I. Volobouev,[24] M. von der Mey,[6] D. Vucinic,[25] R. G. Wagner,[2] R. L. Wagner,[12] W. Wagner,[21] N. B. Wallace,[40] Z. Wan,[40] C. Wang,[11] M. J. Wang,[1] S. M. Wang,[13] B. Ward,[16] S. Waschke,[16] T. Watanabe,[45] D. Waters,[32] T. Watts,[40] M. Weber,[24] H. Wenzel,[21] W. C. Wester III,[12] A. B. Wicklund,[2] E. Wicklund,[12] T. Wilkes,[5] H. H. Williams,[34] P. Wilson,[12] B. L. Winer,[30] D. Winn,[26] S. Wolbers,[12] D. Wolinski,[26] J. Wolinski,[27] S. Wolinski,[26] S. Worm,[40] X. Wu,[15] F. Wuerthwein,[25] J. Wyss,[35] U. K. Yang,[9] W. Yao,[24] G. P. Yeh,[12] P. Yeh,[1] K. Yi,[20] J. Yoh,[12] C. Yosef,[27] T. Yoshida,[31] I. Yu,[22] S. Yu,[34] Z. Yu,[49] J. C. Yun,[12] A. Zanetti,[44] F. Zetti,[24] and S. Zucchelli[3]

(CDF Collaboration)

[1] *Institute of Physics, Academia Sinica, Taipei, Taiwan 11529, Republic of China*

[2] *Argonne National Laboratory, Argonne, Illinois 60439*

[3] *Istituto Nazionale di Fisica Nucleare, University of Bologna, I-40127 Bologna, Italy*

[4] *Brandeis University, Waltham, Massachusetts 02254*

[5] *University of California at Davis, Davis, California 95616*

[6] *University of California at Los Angeles, Los Angeles, California 90024*

[7] *Instituto de Fisica de Cantabria, CSIC-University of Cantabria, 39005 Santander, Spain*

[8] *Carnegie Mellon University, Pittsburgh, PA 15218*

[9] *Enrico Fermi Institute, University of Chicago, Chicago, Illinois 60637*

[10] *Joint Institute for Nuclear Research, RU-141980 Dubna, Russia*

[11] *Duke University, Durham, North Carolina 27708*

[12] *Fermi National Accelerator Laboratory, Batavia, Illinois 60510*

[13] *University of Florida, Gainesville, Florida 32611*

[14] *Laboratori Nazionali di Frascati, Istituto Nazionale di Fisica Nucleare, I-00044 Frascati, Italy*

[15] *University of Geneva, CH-1211 Geneva 4, Switzerland*

[16] *Glasgow University, Glasgow G12 8QQ, United Kingdom*

[17] *Harvard University, Cambridge, Massachusetts 02138*

[18] *Hiroshima University, Higashi-Hiroshima 724, Japan*

[19] *University of Illinois, Urbana, Illinois 61801*

[20] *The Johns Hopkins University, Baltimore, Maryland 21218*

[21] *Institut für Experimentelle Kernphysik, Universität Karlsruhe, 76128 Karlsruhe, Germany*

[22] *Center for High Energy Physics: Kyungpook National University, Taegu 702-701; Seoul National University, Seoul 151-742; and SungKyunKwan University, Suwon 440-746; Korea*

[23] High Energy Accelerator Research Organization (KEK), Tsukuba, Ibaraki 305, Japan
[24] Ernest Orlando Lawrence Berkeley National Laboratory, Berkeley, California 94720
[25] Massachusetts Institute of Technology, Cambridge, Massachusetts 02139
[26] University of Michigan, Ann Arbor, Michigan 48109
[27] Michigan State University, East Lansing, Michigan 48824
[28] University of New Mexico, Albuquerque, New Mexico 87131
[29] Northwestern University, Evanston, Illinois 60208
[30] The Ohio State University, Columbus, Ohio 43210
[31] Osaka City University, Osaka 588, Japan
[32] University of Oxford, Oxford OX1 3RH, United Kingdom
[33] Universita di Padova, Istituto Nazionale di Fisica Nucleare, Sezione di Padova, I-35131 Padova, Italy
[34] University of Pennsylvania, Philadelphia, Pennsylvania 19104
[35] Istituto Nazionale di Fisica Nucleare, University and Scuola Normale Superiore of Pisa, I-56100 Pisa, Italy
[36] University of Pittsburgh, Pittsburgh, Pennsylvania 15260
[37] Purdue University, West Lafayette, Indiana 47907
[38] University of Rochester, Rochester, New York 14627
[39] Rockefeller University, New York, New York 10021
[40] Rutgers University, Piscataway, New Jersey 08855
[41] Texas A&M University, College Station, Texas 77843
[42] Texas Tech University, Lubbock, Texas 79409
[43] Institute of Particle Physics, University of Toronto, Toronto M5S 1A7, Canada
[44] Istituto Nazionale di Fisica Nucleare, University of Trieste/ Udine, Italy
[45] University of Tsukuba, Tsukuba, Ibaraki 305, Japan
[46] Tufts University, Medford, Massachusetts 02155
[47] Waseda University, Tokyo 169, Japan
[48] University of Wisconsin, Madison, Wisconsin 53706
[49] Yale University, New Haven, Connecticut 06520
[*] Now at University of California, Santa Barbara, California 93106

Abstract

We report on measurements of the branching ratios of the decays $B^+ \to \chi^0_{c1}(1P)K^+$ and $B^+ \to J/\psi K^+\pi^+\pi^-$, where $\chi^0_{c1}(1P) \to J/\psi\gamma$ and $J/\psi \to \mu^+\mu^-$ in $p\overline{p}$ collisions at $\sqrt{s} = 1.8$ TeV. Using a data sample from an integrated luminosity of 110 pb^{-1} collected by the Collider Detector at Fermilab we measure the branching ratios to be $BR(B^+ \to \chi^0_{c1}(1P)K^+) = 15.5 \pm 5.4(stat) \pm 1.5(syst) \pm 1.3(br) \times 10^{-4}$ and $BR(B^+ \to J/\psi K^+\pi^+\pi^-) = 6.9 \pm 1.8(stat) \pm 1.1(syst) \pm 0.4(br) \times 10^{-4}$ where (br) is due to the finite precision on $BR(B^+ \to J/\psi K^+)$ and $BR(\chi^0_{c1}(1P) \to J/\psi\gamma)$ used to normalize the signal yield, and $(syst)$ encompasses all other systematic uncertainties.

PACS numbers: 13.85.Ni, 14.40.Gx

1 Introduction

In this paper we report on measurements of the branching ratios of $B^+ \to \chi^0_{c1}(1P)K^+$ and $B^+ \to J/\psi K^+\pi^+\pi^-$ observed in $p\bar{p}$ interactions at a center of mass energy of $\sqrt{s} = 1.8$ TeV. These decay modes were observed in a data sample of an integrated luminosity of 110 pb^{-1}, using the decay channels $\chi^0_{c1}(1P) \to J/\psi\gamma$ and $J/\psi \to \mu^+\mu^-$. Here and throughout this paper, reference to a specific state implies the charge-conjugate state as well. The

current Particle Data Group values for these branching ratios are based on measurements by ARGUS[1, 2] and CLEO[3, 4] using data from e^+e^- colliders operating at the $\Upsilon(4S)$ resonance and have uncertainties of the order of 50%. A more precise measurement based on e^+e^- collider data has recently been published by the BABAR collaboration for the decays $B^+ \to J/\psi K^+$ and $B^+ \to \chi^0_{c1}(1P)K^+$[5].

Theoretical predictions based on factorization and isospin symmetry exist for some hadronic B meson decays to charmonium[6, 7] but have large uncertainties. These results indicate that decays with a spin 1 charmonium particle in the final state, such as $B^+ \to J/\psi K^+$ and $B^+ \to \chi^0_{c1}(1P)K^+$ have branching ratios of similar magnitude[6]. At CDF the $\chi^0_{c1}(1P)$ decay to $J/\psi\gamma$ is indistinguishable from the corresponding $\chi^0_{c2}(1P)$ decay due to the resolution of the calorimeter[8], but the decay $B^+ \to \chi^0_{c2}(1P)K^+$ is forbidden if soft gluon exchange is neglected[1, 9, 10].

Since the process $B^+ \to J/\psi K^+$ is similar to the processes we want to measure, and its branching ratio is comparatively well measured, a ratio of branching ratios was measured between the signal ("sig") modes $B^+ \to \chi^0_{c1}(1P)K^+$ and $B^+ \to J/\psi K^+\pi^+\pi^-$ and the well established reference ("ref") mode $B^+ \to J/\psi K^+$. Many systematic uncertainties cancel in this ratio which is given by equation 1.

$$\frac{BR_{sig}}{BR_{ref}} = C\left(\frac{N_{sig}}{N_{ref}}\right)\left(\frac{A_{ref}}{A_{sig}}\right) \tag{1}$$

The number of observed events, N_{sig} and N_{ref}, were measured in the data while applying similar selection criteria to both signal and reference decay modes. The acceptances A_{sig} and A_{ref} were calculated with a Monte Carlo simulation and additional information from the data as discussed later in this paper. The term C is equal to one for the decay $B^+ \to J/\psi K^+\pi^+\pi^-$ and $1/BR(\chi^0_{c1}(1P) \to J/\psi\gamma)$ for the decay $B^+ \to \chi^0_{c1}(1P)K^+$.

2 The CDF Detector

The data were collected in the periods 1992-93 (Run 1A) and 1993-95 (Run 1B) by the Collider Detector at Fermilab (CDF). The CDF detector has been described in detail elsewhere [11, 12]. The components most relevant to this analysis are briefly described here. A cylindrical coordinate system (r, ϕ, z) best defines the CDF detector where the proton beam defines the $+z$ direction, r is the transverse distance from the beam axis, and ϕ is the azimuthal angle. The pseudorapidity is defined as $\eta \equiv -\ln[\tan(\theta/2)]$ and the momentum component transverse to the beam axis is denoted by p_T. The Central Tracking Chamber (CTC) and Silicon Vertex detector (SVX) were placed in a 1.4 T axial magnetic field. The CTC had a resolution of $\delta p_T/p_T = \sqrt{(0.0011p_T)^2 + (0.0066)^2}$ for tracks constrained to come from the beam line, where p_T is measured in GeV/c. The SVX provided high resolution tracking information close to the nominal $p\bar{p}$ interaction point for improved vertexing. The central electromagnetic and hadronic calorimeters located outside the tracking volume were constructed with a projective tower geometry which pointed toward the nominal $p\bar{p}$ interaction point and covered the region $|\eta| < 1.1$. The calorimeter towers subtended approximately 0.1 in η by 15° in ϕ. A system of proportional chambers (CES) was embedded in the electromagnetic calorimeter at a depth of six radiation lengths for measuring the position of the electromagnetic showers at the stage of maximum development. The central muon chambers (CMU), at a radius of 3.5 m from the beam axis, were located behind the calorimeter and provided muon identification in the region of pseudorapidity $|\eta| < 0.6$. The

central muon upgrade system (CMP) which consisted of four layers of drift chambers was located outside the CMU behind an additional four interaction lengths of steel absorber and covered a similar region of η. Finally, the CMX muon system extended the coverage up to $|\eta| < 1.0$. Depending on the incident angle, particles had to penetrate six to nine absorption lengths of material to be detected in the CMX.

3 Event Selection

The measurements reported here are based on a data sample of muon pairs collected with a three-level online trigger. The first level trigger required two charged track segments in the central muon chambers. The efficiency for this trigger rises from ∼40% at $p_T = 1.5$ GeV/c to 93% for muons with $p_T > 3.0$ GeV/c. At the second level at least one muon segment was required to match a CTC track found by a hardware fast track processor (CFT). The CFT performed a partial reconstruction of all charged tracks with p_T above 2 GeV/c. Muon candidates found by the first level trigger were required to match a CFT track extrapolated to the muon chambers within about 15 degrees in azimuth. The third level trigger required that two reconstructed CTC tracks be matched with two tracks in the muon chambers and that the invariant mass of the dimuon pair be between 2.7 and 4.1 GeV/c^2.

Additional requirements were made offline to suppress background in the dimuon sample. Each muon chamber track was required to match its associated CTC track to within 3σ in $r - \phi$ and 3.5σ in z, where σ is the calculated uncertainty due to multiple scattering, energy loss, and measurement uncertainties. Muons from the $J/\psi \to \mu^+\mu^-$ decay were required to be identified by the CMU alone or both the CMU and CMP for tracks with $|\eta| < 0.6$. Muons with $0.6 < |\eta| < 1.0$ were required to be identified by the CMX system. The muons were also required to have opposite charge. The p_T of each muon from the J/ψ, for Run 1A, was required to be greater than 2.0 GeV/c with one muon of the pair greater than 2.8 GeV/c. For Run 1B, due to different trigger thresholds, both muons were required to have p_T greater than 2.0 GeV/c. J/ψ events were selected by requiring that the muon pair forms a vertex and has an invariant mass within ± 40 MeV/c^2 from the world average value for $m_{J/\psi}$[13].

The resulting J/ψ muon tracks were then combined with other tracks to reconstruct the B^+ decay vertex. For both the $B^+ \to \chi^0_{c1}(1P)K^+$, $\chi^0_{c1}(1P) \to J/\psi\gamma$, $J/\psi \to \mu^+\mu^-$ and $B^+ \to J/\psi K^+\pi^+\pi^-$, $J/\psi \to \mu^+\mu^-$ decay chains, the dimuon mass was constrained to the world average value for $m_{J/\psi}$ during the fit. At least one of the muon tracks as well as all of the other tracks were required to have hits in the SVX in order to use well measured tracks close to the $p\bar{p}$ interaction point and thus ensure good vertex parameter measurements. For $B^+ \to J/\psi K^+\pi^+\pi^-$ decays the events for which the invariant mass of the $J/\psi\pi^+\pi^-$ was within 10 MeV/c^2 of the ψ(2S) mass were removed in order to exclude the decay $B^+ \to \psi(2S)K^+$ where $\psi(2S) \to J/\psi\pi^+\pi^-$. Track combinations with a vertex fit χ^2 probability greater than 1% were then included in the B^+ mass fits.

To reconstruct $B^+ \to \chi^0_{c1}(1P)K^+$ candidates where the $\chi^0_{c1} \to J/\psi\gamma$, we selected events with a $J/\psi K^+$ vertex and a transverse energy deposition of at least 0.7 GeV in a cell of the central electromagnetic calorimeter with a signal in the fiducial volume of the CES chambers. The fiducial volume requirement ensured that the shower was fully contained in a cell. The location of the signal in the CES chambers and the reconstructed $J/\psi K^+$ vertex determine the direction of the photon momentum; its magnitude is the energy deposited in

the calorimeter. We retained photon candidates that had no tracks extrapolating to their calorimeter cell. Figure 1 shows the measured $M_{J/\psi\gamma} - m_{\chi_{c1}(1P)}$ spectrum. To identify events with a $\chi^0_{c1}(1P)$ the reconstructed $M_{J/\psi\gamma}$ was required to be within ± 110 MeV/c^2 of the world average value for $m_{\chi_{c1}(1P)}$[13]. The identified $\chi^0_{c1}(1P)$ events were then included in the $\chi^0_{c1}(1P)K^+$ invariant mass distribution where the $J/\psi\gamma$ mass has been constrained to the world average value for $m_{\chi_{c1}(1P)}$.

To reduce background levels, additional selection criteria were placed on the p_T of the non-J/ψ tracks, the p_T of the B meson candidate, the proper decay length of the B^+ candidate, $ct(B)$, the impact parameter of the B^+ momentum with respect to the beam line, $|I_{xy}(B)|$, and the B^+ isolation variable $f_{p_T} = p_T(B)/(p_T(B) + \sum p_T^{cone})$. The quantity $\sum p_T^{cone}$ is the scalar sum of the transverse momenta of all non-B^+ candidate tracks within $\sqrt{(\Delta\eta)^2 + (\Delta\phi)^2}$ <1.0 of the B^+ momentum direction. For each signal mode the selection criteria were optimized to maximize $S^2/(S + Bkg)$ of the signal sample where S is the expected signal for 110 pb^{-1}, and Bkg is the background underneath the signal. S was calculated using the acceptances from the Monte Carlo and inverting equation (1) to find $S \equiv N_{sig}^{expected} = N_{ref}(BR_{sig}/BR_{ref})(A_{sig}/A_{ref})$. Bkg was derived from fits to the sidebands around the signal peak observed in data. The optimized cuts are listed in table I. The optimization of $ct(B)$ and $|I_{xy}(B)|$ yielded similar results for the two analyses, whereas the optimization of the p_T cuts and f_{p_T} were different for the two analyses due to the different numbers of particles in the final states.

4 Candidate B Meson Invariant Mass Distributions

The resulting $\chi^0_{c1}(1P)K^+$ and $J/\psi K^+\pi^+\pi^-$ mass distributions are shown in figures 2 and 3 respectively. The $\chi^0_{c1}(1P)K^+$ mass distribution is fit with a gaussian for the signal and a first order polynomial for the background. The $J/\psi K^+\pi^+\pi^-$ mass distribution is fit with two gaussians of equal area for the signal and a first order polynomial for the background. Since we cannot adequately distinguish between kaons and pions, figure 3 has two entries per event. The second gaussian is used to account for incorrect assignment for the kaon and pion tracks. The width of the gaussians used in the fit for both decays is fixed based on the width measured in the Monte Carlo scaled by the difference in widths observed between data and Monte Carlo for the reference signal $J/\psi K^+$. For all fits the mean of the gaussian was a free parameter. The reference signal $J/\psi K^+$ is shown in figure 4 using the final kinematic cuts used by the $B^+ \to \chi^0_{c1}(1P)K^+$ analysis. The fits of the $\chi^0_{c1}(1P)K^+$ and $J/\psi K^+$ mass distributions exclude the region below 5.15 GeV/c^2 to avoid including partially reconstructed $B \to J/\psi K^*$ events. The values for N_{sig} and N_{ref} are summarized in table II.

5 Efficiency Corrections

A Monte Carlo simulation was used to optimize the kinematic cuts described above as well as calculate efficiency corrections. For this simulation a mix of B^+ and B^- events were simulated based on the NLO QCD predictions of Nason, Dawson, and Ellis (NDE)[14, 15]. The input parameters to the model were set to a renormalization and factorization scale of $\mu = \mu_0 = \sqrt{m_b^2 + p_T^2}$, mass of the b quark $m_b = 4.75$ GeV/c^2, and Peterson fragmentation parameter $\epsilon = 0.006$. Events in the channel $B^+ \to J/\psi K^+$ were generated for calculating the geometrical acceptance A_{ref}. Events in the channels $B^+ \to \chi^0_{c1}(1P)K^+$

and $B^+ \to J/\psi K^+\pi^+\pi^-$ were generated for estimating the signal acceptances $A_{\chi^0_{c1}(1P)K^+}$ and $A_{J/\psi K^+\pi^+\pi^-}$ for use in equation (1).

Both the acceptances $A_{\chi^0_{c1}(1P)K^+}$ and $A_{J/\psi K^+\pi^+\pi^-}$ were calculated using the factorized forms described below.

$$A_{\chi^0_{c1}(1P)K^+} = A^{geom}_{J/\psi K^+} \times A^{\gamma} \qquad A_{J/\psi K^+\pi^+\pi^-} = A^{geom}_{J/\psi K^+\pi^+\pi^-} \times A^{track} \tag{2}$$

The $\chi^0_{c1}(1P)K^+$ acceptance is assumed to factorize into a geometrical term similar to the acceptance for the reference signal and a photon term. The $J/\psi K^+\pi^+\pi^-$ acceptance is assumed to factorize into a geometrical term and a tracking efficiency term due to the two extra pion tracks with respect to the reference signal.

The two geometrical acceptances, $A^{geom}_{J/\psi K^+}$ and $A^{geom}_{J/\psi K^+\pi^+\pi^-}$ were both calculated using the Monte Carlo simulation in the kinematic range $p_T^{min} < p_T^B < 30.0$ GeV/c and $|y_B| < 0.9$ where $p_T^{min} = 5.0$ GeV/c for the $\chi^0_{c1}(1P)K^+$ analysis and $p_T^{min} = 6.0$ GeV/c for the $J/\psi K^+\pi^+\pi^-$ analysis as described in the section on event selection, and y_B is the rapidity of the B meson. The J/ψ from the decay $\chi^0_{c1}(1P) \to J/\psi\gamma$ was generated unpolarized using the assumption of a purely electric dipole transition [16, 17]. The photon acceptance, A^{γ}, is the product of the probability that the photon is within the fiducial volume, the reconstruction efficiency of the fiducial photon, and the probability that there is no track in the photon tower. The fiducial probability was calculated using the Monte Carlo simulation. The photon reconstruction efficiency was obtained from real data by applying the photon requirements to a sample of electrons from photon conversions selected using only tracking information[18, 19]. The "no track" probability was estimated by looking at the track occupancy of calorimeter towers in the data for $B^+ \to J/\psi K^+$ events. The tracking efficiency, A^{track}, was estimated by combining the p_T spectrum for the two pions from Monte Carlo with the measured pion tracking efficiency[20] in bins of p_T. The values of the acceptances and their factorized parts are summarized in table II.

6 Systematic Uncertainties

Both branching ratio measurements have a systematic error due to the uncertainty on the world average value of $BR(B^+ \to J/\psi K^+)$ used to extract the absolute branching ratios. Since they both used the same Monte Carlo generation algorithm, they also share an uncertainty due to the B production model used. These effects were estimated by varying the scale by a factor of two above and below the central value of $\mu = \mu_0$, varying the b quark mass by ± 0.25 GeV/c^2 around the central value of 4.75 GeV/c^2, and varying the Peterson fragmentation parameter by ± 0.002 around the central value of 0.006. The difference between the largest and smallest values for the ratio A_{ref}/A_{sig} was used to estimate the uncertainty on the branching ratio.

The systematic uncertainties specific to the $B^+ \to J/\psi K^+\pi^+\pi^-$ decay channel are primarily due to acceptance uncertainties. In addition to purely fiducial effects, the value of $A^{geom}_{J/\psi K^+\pi^+\pi^-}$ may be affected by mass resonances and helicity effects. The primary mass resonances affecting the above decay are $B^+ \to J/\psi K_2^{*+}$, $K_2^{*+} \to K^{*0}\pi^+$, $K^{*0} \to K^+\pi^-$ and $B^+ \to J/\psi K^{*0}\pi^+$, $K^{*0} \to K^+\pi^-$. These processes were simulated using the Monte Carlo and the difference between the maximum and minimum values for $A^{geom}_{J/\psi K^+\pi^+\pi^-}$ was used to estimate the uncertainty. The effect of helicities was simulated by generating events with the daughter particles polarized either longitudinally or transversely. Half of the

difference between the $A^{geom}_{J/\psi K^+\pi^+\pi^-}$ values for the two helicity states was used to estimate the uncertainty. Since the $J/\psi K^+\pi^+\pi^-$ vertex is formed from five tracks rather than the three used for the reference signal, an uncertainty due to vertex efficiency is included for that channel. The uncertainty due to tracking efficiency was found to be negligible.

The systematics specific to the $B^+ \to \chi^0_{c1}(1P)K^+$ decay channel are related to uncertainties on the photon acceptance. Since the photon detection efficiency is determined using conversion electrons, there is an uncertainty in the estimation of the detector response between photons and electrons, due to the uncertainty on the amount of material in front of the calorimeter. There is also an uncertainty on the "no track" isolation efficiency which is simply statistical in nature. Based on the result in reference [17] and the results of the Monte Carlo simulation, we concluded that the uncertainty due to J/ψ helicity was negligible for this decay. The individual systematic errors are summarized in table III.

7 Conclusion

The measured values for BR_{sig}/BR_{ref} are $1.53 \pm 0.53(stat) \pm 0.15(syst) \pm 0.09(br)$ and $0.68 \pm 0.18(stat) \pm 0.11(syst)$ for the decays $B^+ \to \chi^0_{c1}(1P)K^+$ and $B^+ \to J/\psi K^+\pi^+\pi^-$, respectively. The third uncertainty for the $B^+ \to \chi^0_{c1}(1P)K^+$ ratio is due to the uncertainty on $BR(\chi^0_{c1}(1P) \to J/\psi\gamma) = 0.273 \pm 0.016$[13]. As expected, the ratios are close to unity[6]. The final branching ratios were extracted using the value measured by the BABAR collaboration of $BR(B^+ \to J/\psi K^+) = 10.1 \pm 0.6 \times 10^{-4}$[5] which gave the results $BR(B^+ \to \chi^0_{c1}(1P)K^+) = 15.5 \pm 5.4(stat) \pm 1.5(syst) \pm 1.3(br) \times 10^{-4}$ and $BR(B^+ \to J/\psi K^+\pi^+\pi^-) = 6.9 \pm 1.8(stat) \pm 1.1(syst) \pm 0.4(br) \times 10^{-4}$. The uncertainty on BR_{ref} has been added in quadrature to the (br) part of the error for both measurements. Our measurements are consistent with, and have a similar precision to, the corresponding world averages of $10 \pm 4 \times 10^{-4}$ and $14 \pm 6 \times 10^{-4}$[13]. These also represent the first measurements of these branching ratios at a hadron collider. The measurement for $BR(B^+ \to \chi^0_{c1}(1P)K^+)$ can also be compared to the recent measurement by the BABAR collaboration of $7.5 \pm 0.8(stat) \pm 0.8(syst) \times 10^{-4}$[5] which is consistent with our result but with better precision.

8 Acknowledgements

We thank the Fermilab staff and the technical staffs of the participating institutions for their vital contributions. This work was supported by the U.S. Department of Energy and National Science Foundation; the Italian Istituto Nazionale di Fisica Nucleare; the Ministry of Education, Science and Culture of Japan; the Natural Sciences and Engineering Research Council of Canada; the National Science Council of the Republic of China; the Swiss National Science Foundation; the A. P. Sloan Foundation; the Bundesministerium für Bildung und Forschung, Germany; the Korea Science and Engineering Foundation (KoSEF); the Korea Research Foundation; and the Comision Interministerial de Ciencia y Tecnologia, Spain.

References

[1] H. Albrecht *et al.*, ARGUS Collaboration, Phys.Lett. **B277**, 209 (1992)

[2] H. Albrecht *et al.*, ARGUS Collaboration, Z. Phys. **C48**, 543 (1990)

[3] M.S. Alam *et al.*, CLEO Collaboration, Phys.Rev. **D50**, 43 (1994)

[4] D. Bortoletto *et al.*, CLEO Collaboration, Phys.Rev. **D45**, 21 (1992)

[5] B. Aubert *et al.*, BABAR Collaboration, Phys. Rev. **D65**, 032001, (2002).

[6] M. Gourdin, Y. Y. Keum, X. Y. Pham, Phys. Rev. D **52**, 1597 (1995).

[7] H. Y. Cheng and K. C. Yang, Phys. Rev. D **63**, 074011 (2001).

[8] T. Affolder *et al.*, CDF Collaboration, Phys. Rev. Lett. **86**, 3963 (2001).

[9] J. H. Kuehn, S. Nussinov and R. Ruckl, Z. Phys. **C5** 117 (1980).

[10] J. H. Kuehn and R. Ruckl, Phys. Lett. **B135**, 477 (1984).

[11] F. Abe *et al.*, CDF Collaboration, Nucl. Instrum. Methods A **271**, 387 (1988).

[12] F. Abe *et al.*, CDF Collaboration, Phys. Rev. **D50**, 2966 (1994).

[13] C. Caso *et al.*, Particle Data Group, Eur. Phys. J **C15**, 1 (2000).

[14] P. Nason, S. Dawson, and R. K. Ellis, Nucl. Phys. **B327**, 49 (1989).

[15] P. Nason, S. Dawson, and R. K. Ellis, Nucl. Phys. **B303**, 607 (1988).

[16] A. D. Martin *et al.*, Phys. Lett. **B147**, 203 (1984).

[17] M. Oreglia *et al.*, Phys. Rev. **D25**, 2259, (1982).

[18] T. Affolder *et al.*, CDF Collaboration, Phys. Rev. Lett. **84**, 2094 (2000).

[19] F. Abe *et al.*, CDF Collaboration, Phys. Rev. Lett. **79**, 578 (1997).

[20] D. Acosta *et al.*, CDF Collaboration, FERMILAB-PUB-01/327-E, submitted to Phys. Rev. **D**.

Table I: Summary of optimized kinematic cuts.

	$B^+ \to \chi^0_{c1}(1P)K^+$	$B^+ \to J/\psi K^+\pi^+\pi^-$
$ct(B)$	$> 80\mu$m	$> 80\mu$m
$\lvert I_{xy}(B)\rvert$	$< 100\mu$m	$< 100\mu$m
f_{p_T}	> 0.6	> 0.7
$p_T(B)$	> 5 GeV/c	> 6 GeV/c
$p_T(K,\pi)$	> 1.25 GeV/c	> 0.7 GeV/c

Table II: Summary of quantities used to calculate the ratio of branching ratios. Note that the acceptances for the two decay channels use different minimum p_T requirements for the B meson and are not directly comparable. All uncertainties are statistical only.

	$B^+ \to \chi^0_{c1}(1P)K^+$	$B^+ \to J/\psi K^+\pi^+\pi^-$
N_{ref}	525 ± 27	435 ± 28
N_{sig}	19.8 ± 6.8	56.7 ± 14.5
A_{ref}	0.0467 ± 0.0006	0.0694 ± 0.0003
A_{sig}	0.00417 ± 0.00022	0.0131 ± 0.0010
A^{geom}	0.0276 ± 0.0004	0.0132 ± 0.0001
A^{track}	–	0.990 ± 0.004
A^{γ}	0.151 ± 0.004	–

Table III: Systematic uncertainties on $BR(B^+ \to \chi^0_{c1}(1P)K^+)$ and $BR(B^+ \to J/\psi K^+\pi^+\pi^-)$

Source of Uncertainty	$BR(B^+ \to \chi^0_{c1}(1P)K^+)$	$BR(B^+ \to J/\psi K^+\pi^+\pi^-)$
$BR(B^+ \to J/\psi K^+)$	6.0%	6.0%
$BR(\chi^0_{c1}(1P) \to J/\psi\gamma)$	5.9%	–
B Production Model	9.0%	7.2%
B Decay Model (Resonance)	–	6.6%
B Decay Model (Helicity)	–	13.1%
Vertex Probability	–	3.0%
Photon Eff.	3%	–
Photon-No Track Eff.	3%	–

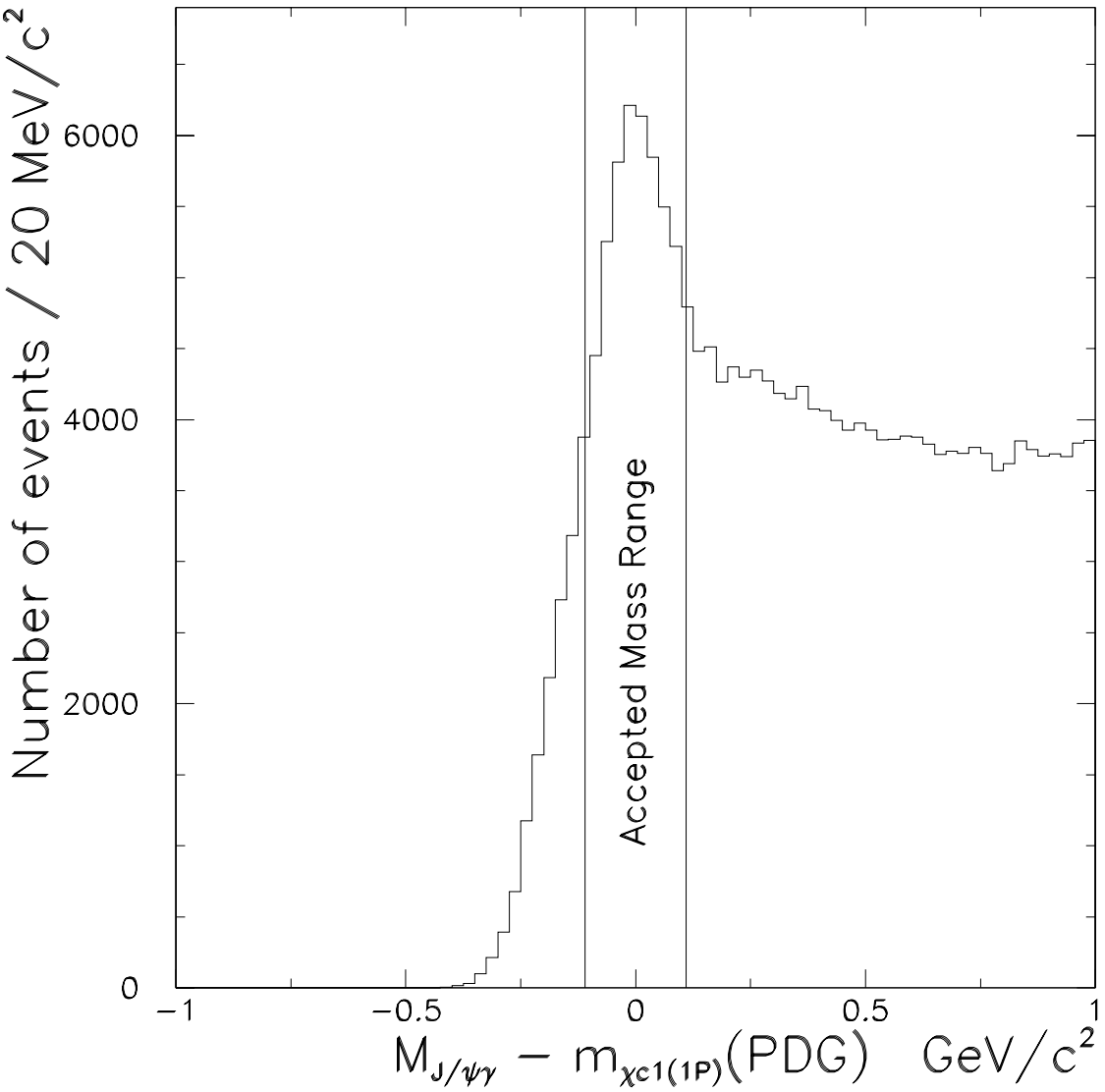

Figure 1: The distribution of the mass difference $[\Delta M = M_{J/\psi\gamma} - m_{\chi_{c1}(1P)}(PDG)]$. The E_T^γ is required to be greater than 0.7 GeV. The measured $M_{J/\psi\gamma}$ is corrected for a 20 MeV/c^2 underestimate due to the calorimeter calibration.

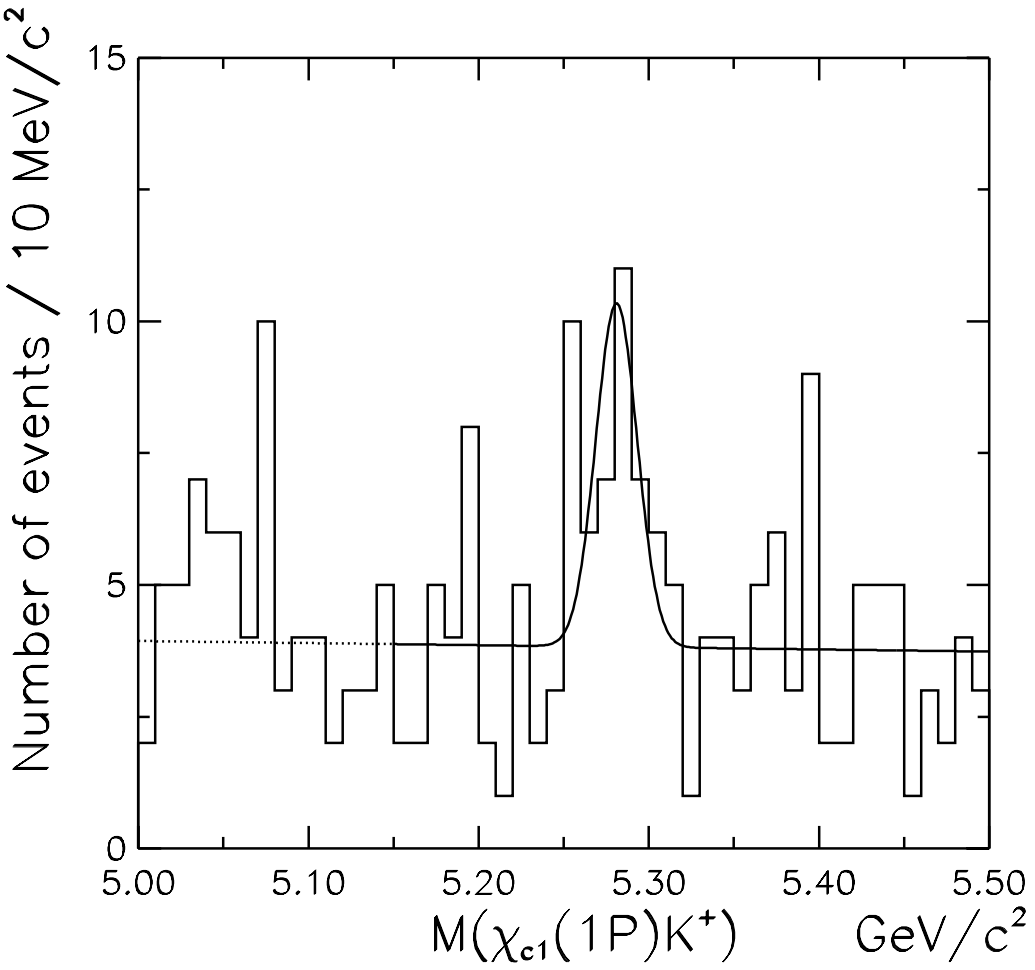

Figure 2: The invariant mass distribution of $\chi^0_{c1}(1P)K^+$ candidate events. The histogram is fitted with a gaussian signal and a linear background with the width of the gaussian fixed to 12.1 MeV/c^2. The peak contains 19.8 ± 6.8 $B^+ \to \chi^0_{c1}(1P)K^+$ events.

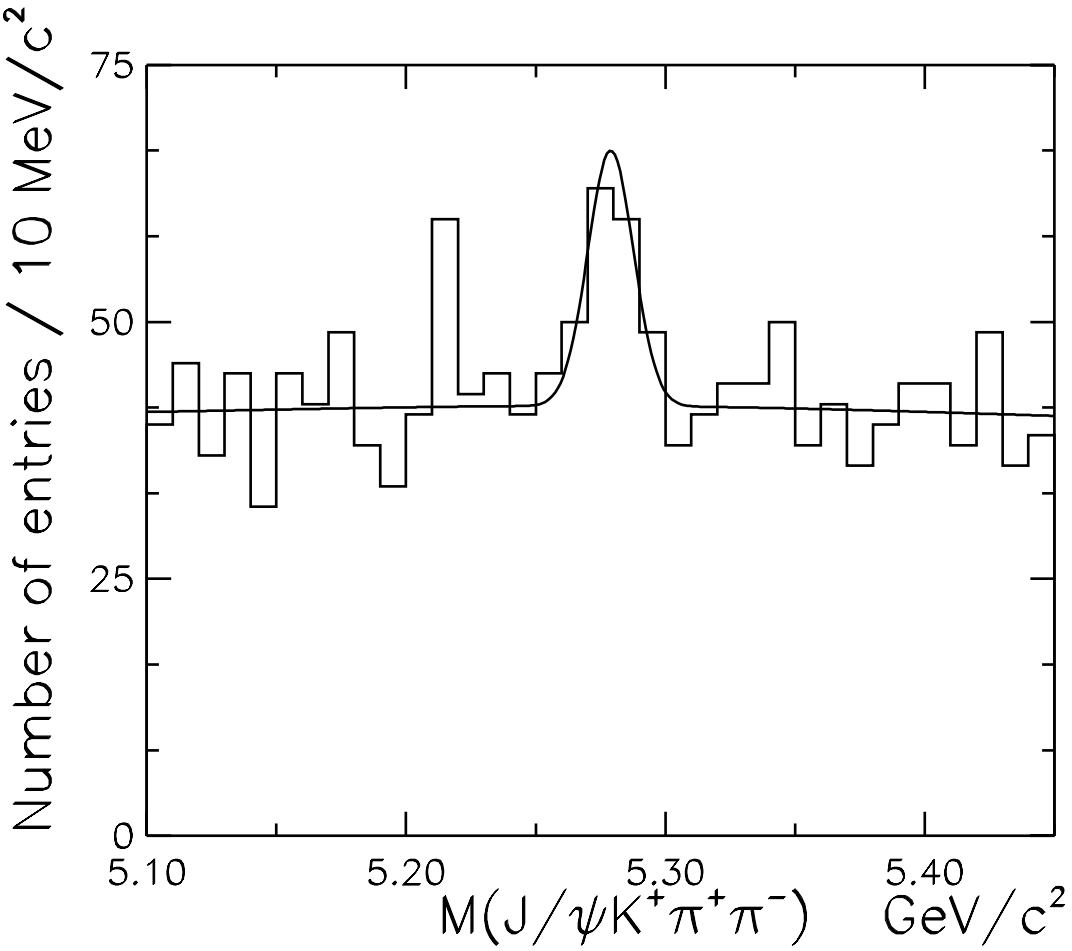

Figure 3: The invariant mass distribution of $J/\psi K^+\pi^+\pi^-$ from Run I data. The histogram is fitted with two gaussians of equal area for the signal and a first order polynomial for the background. The two gaussians are used to account for the ambiguity on the mass of the two same charge meson tracks. The width of the first signal gaussian is fixed to 8.8 MeV/c^2 while the width of the second gaussian is 145 MeV/c^2. The peak contains 56.7 ± 14.5 $B^+ \to J/\psi K^+\pi^+\pi^-$ events.

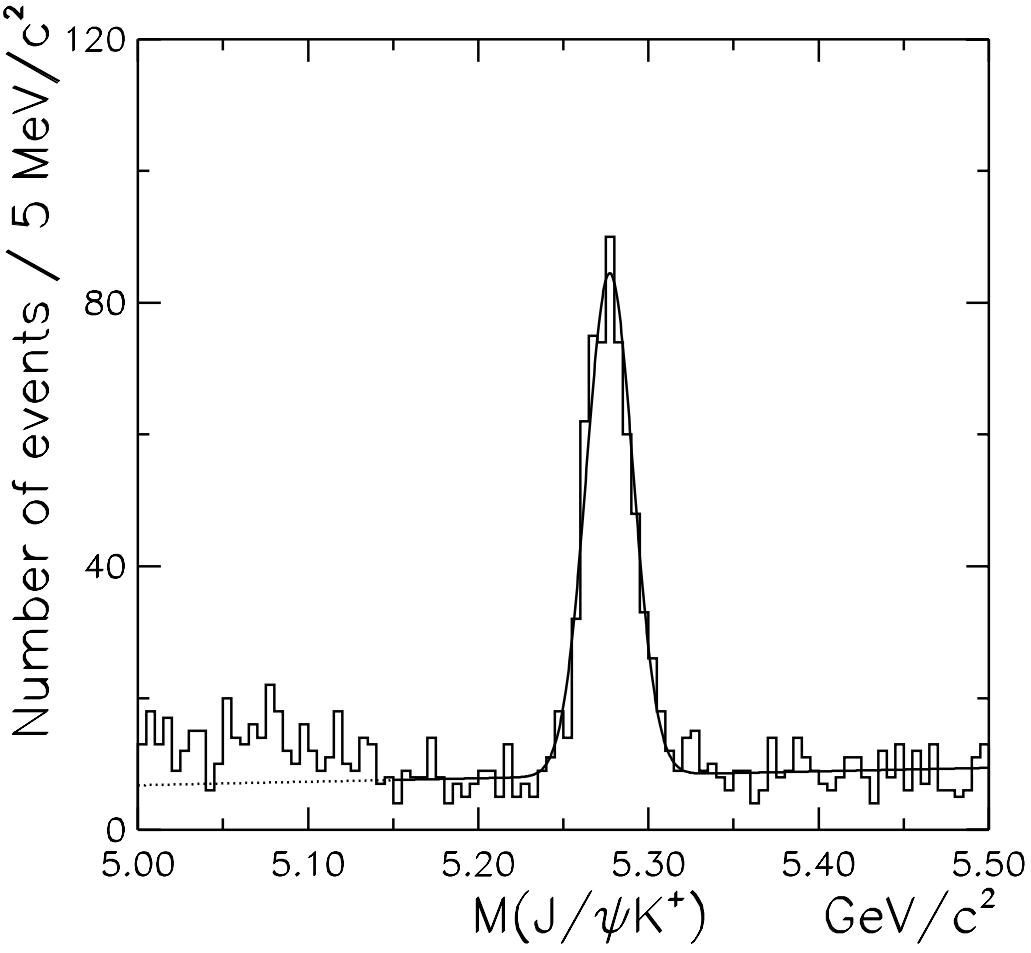

Figure 4: The invariant mass distribution of $J/\psi K^+$ candidate events. The histogram is fitted with a gaussian signal and a linear background. The peak contains 525 ± 25 $B^+ \to J/\psi K^+$ events with a fitted width of 13.2 MeV/c^2.